Supporting Information

Interfacial strength and surface damage characteristics of atomically-thin h-BN, MoS_2 and graphene

Bien-Cuong Tran Khac,[a] *Frank W. DelRio,*[b] *and Koo-Hyun Chung*[*,a]

[a] School of Mechanical Engineering, University of Ulsan, Ulsan 44610, Republic of Korea

[b] Applied Chemicals and Materials Division, Material Measurement Laboratory, National Institute of Standards and Technology, Boulder, Colorado 80305, USA

*Corresponding author: Prof. Koo-Hyun Chung, School of Mechanical Engineering, University of Ulsan; 93 Daehak-ro, Nam-gu, Ulsan 44610, South Korea; Tel: +82-52-259-2744; Fax: +82-52-259-1680; Email: khchung@ulsan.ac.kr

1. Thickness and surface roughness characterization of atomically-thin specimens

Thicknesses of single- and multi-layer h-BN, MoS_2, and graphene specimens with respect to number of layers as shown in Figure S1(a) clearly demonstrate the linear dependence between thickness and number of layers. The interlayer spacing values of h-BN, MoS_2, and graphene were estimated to be about 0.35 nm, 0.64 nm, and 0.37 nm, respectively, which are consistent with their respective theoretical values. Moreover, Figure S1(b) shows the variation of average surface roughness values of h-BN, MoS_2 and graphene specimens with respect to the number of layers. Surface roughness values were determined from AFM topographic images obtained at five different locations with a 1 μm × 1 μm scanning area. Surface roughness values for single-layer h-BN, MoS_2, and graphene were determined to be about 0.16 nm, 0.14 nm, and 0.15 nm, which clearly shows the atomically-flat surfaces of the single-layer specimens used in this work. In addition, the surface roughness of these single-layer specimens were found to be close to that of the SiO_2 substrate (≈ 0.17 nm), suggesting good flexibility and conformity to the underlying substrate. As the number of layers increased, the surface roughness decreased. This behavior is likely due to an increase in bending rigidity as the number of layers increase, which leads to a less dominant effect of the substrate roughness on the morphology of the atomically-thin specimens.

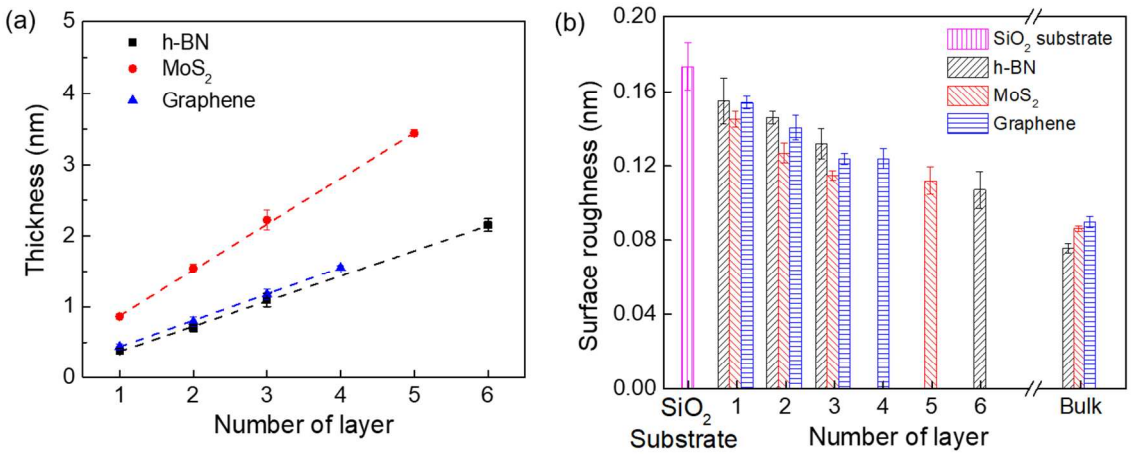

Figure S1. (a) Thickness and (b) surface roughness of atomically-thin h-BN, MoS_2 and graphene specimens with respect to the number of layers. The error bars represent one standard deviation of the mean.

2. Photoluminescence (PL) measurements of single-layer MoS_2

In the recent study, Nan *et al.*[1] observed a strong PL enhancement in single-layer MoS_2 at defects formed during thermal annealing at high temperature. In that study, the authors demonstrated that oxygen chemical adsorption at defect sites, which resulted in the formation of Mo-O bonding, was the main reason for the significant enhancement of both the PL A- and B-excitons at defect sites of single-layer MoS_2. The strong A exciton (≈ 1.84 eV) and the weaker B exciton (≈ 1.98 eV) arise from the direct transition at the K and K' point in the Brillouin zone, respectively.[2]

Figure S2 (a) shows a PL A-exciton intensity map for single-layer MoS_2 specimens after scratch tests at 2000 nN normal force. An intensity decrease is clearly observed in the scratched area. PL spectra obtained at scratched areas under various normal forces as shown in Figure S2(b) demonstrate the gradual intensity decrease of A- and B-excitons with increasing normal force. The results suggest a lack of Mo-O bonding induced by chemically-adsorbed oxygen at the scratched areas.

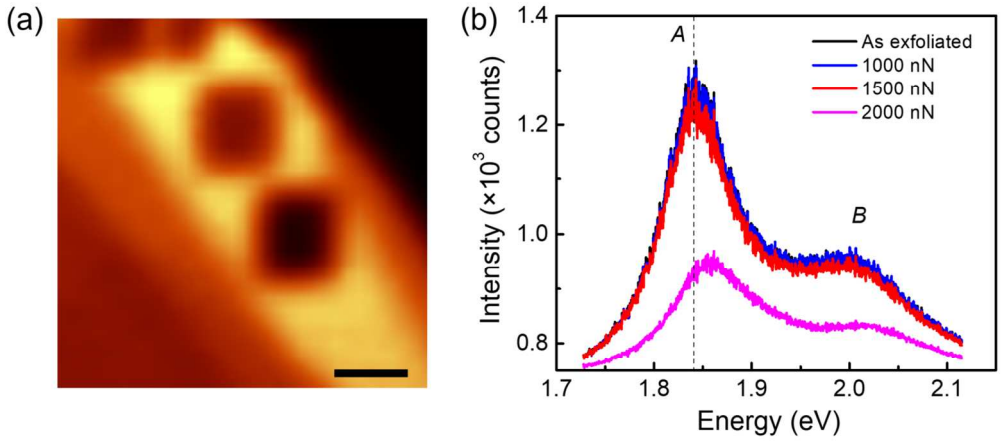

Figure S2. (a) PL intensity image of single-layer MoS_2 after constant-force scratch tests at 2000 nN normal force. (b) PL spectra as a function of normal force. The energy of the A exciton for as-exfoliated single-layer MoS_2 is denoted by a dashed line for comparison. In (a), the scale bar is 1 μm.

3. Raman spectroscopy measurements of scratch tested single-layer graphene

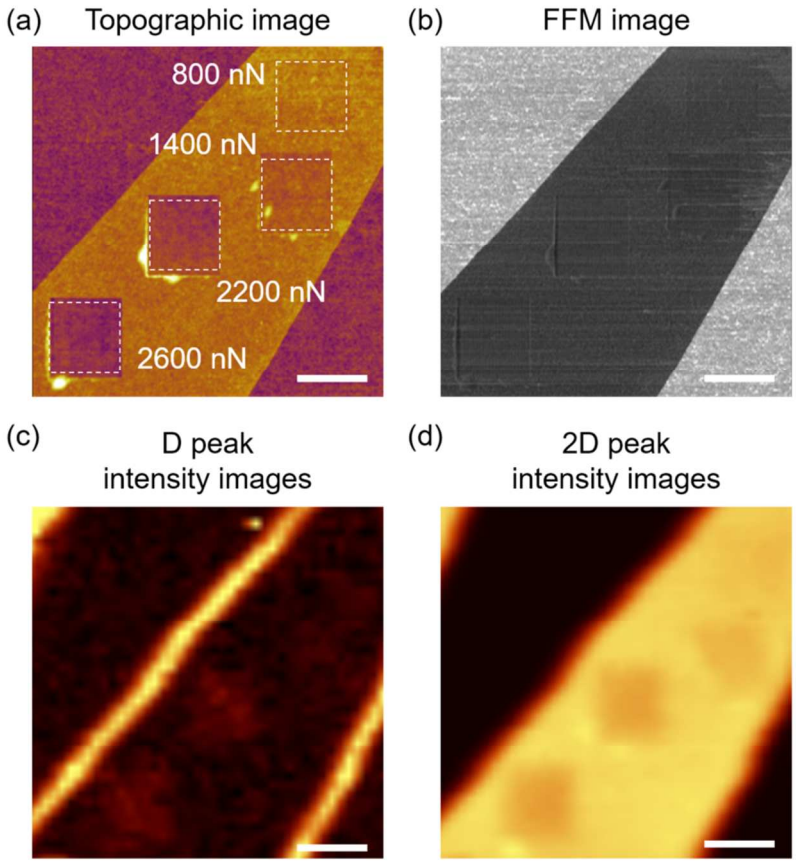

Figure S3. (a) Topographic image, (b) FFM image (forward scan), and Raman images for the (c) D and (d) 2D peak intensities of single-layer graphene after constant force scratch test at normal forces ranging from 800 nN to 2400 nN. The specimens were scratched at a constant normal force in the scratch area of 1 μm × 1 μm, as indicated by the white dashed squares in (a). The scale bars are 1 μm.

4. Compressive strain-induced buckling of atomically-thin specimens

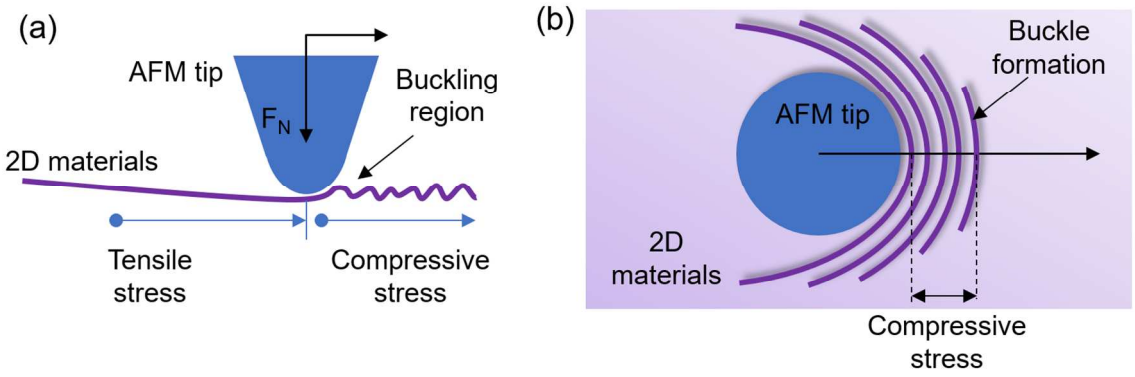

Figure S4. Schematic illustrating the buckling region in front of the sliding AFM tip from (a) side view and (b) plane view during scratch testing.

5. Effect of number of layers on progressive-force scratch tests

To further examine the effect of the number of layers on film-to-substrate interfacial strength, progressive-force scratch tests were performed on multi-layer h-BN, MoS_2 and graphene. The variation in friction force with normal force during the progressive-force scratch tests, and the topographic and FFM images of scratches for multi-layer h-BN, MoS_2 and graphene are shown in Figures S5, S6, and S7, respectively. From this data, the critical forces were determined.

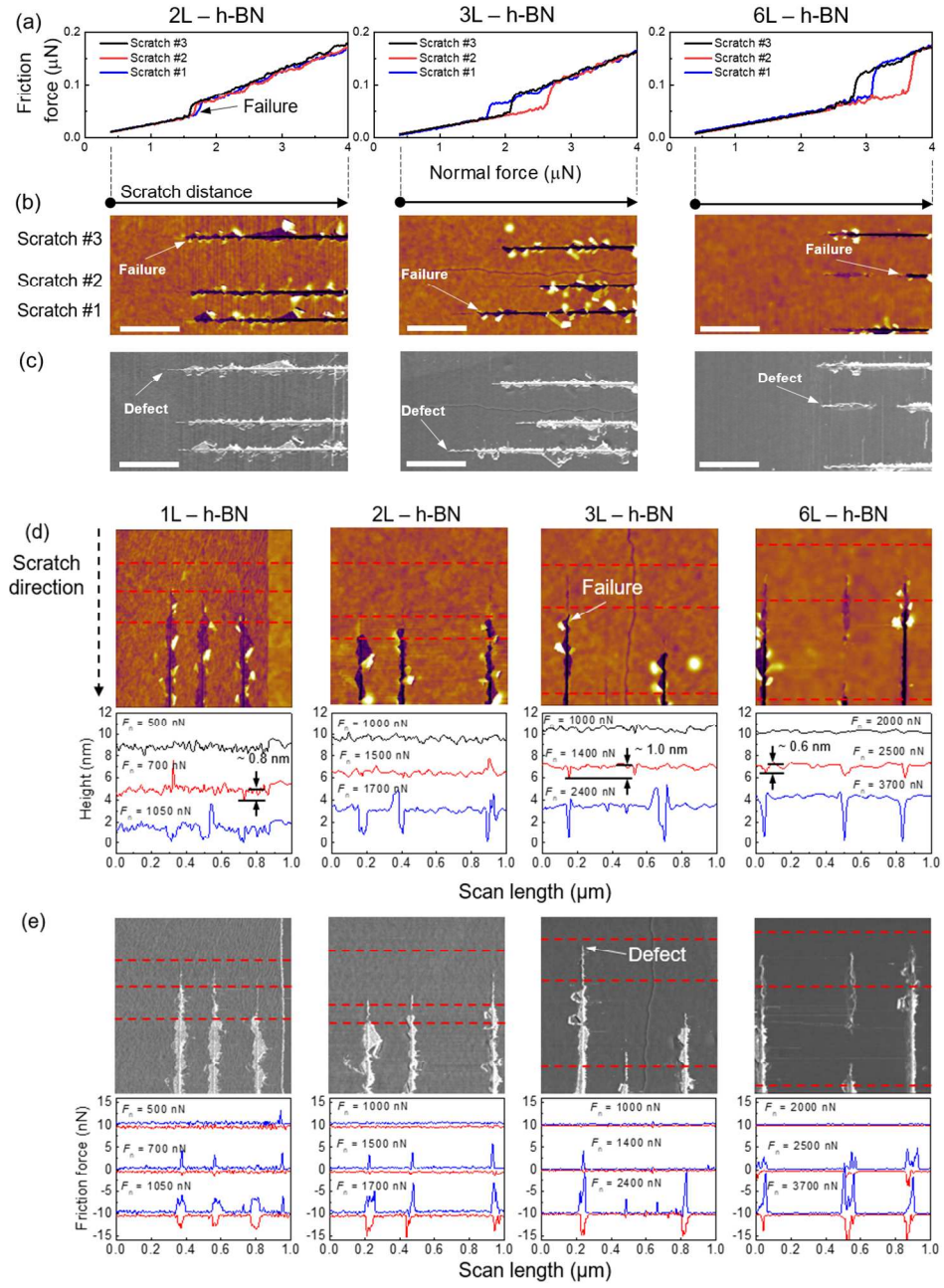

Figure S5. Progressive-force scratch test results for multi-layer h-BN specimens. (a) Friction force variation with respect to normal force, (b) topographic images, and (c) FFM images (forward scans) of scratch tracks after progressive-force scratch tests. In (b), the scratch distance of about 2 μm is noted. In (b) and (c), the scale bars are 500 nm. High-resolution (d) topographic images and (e) FFM images (forward scans) of scratch tracks formed at single- and multi-layer h-BN specimens after progressive-force scratch tests. The cross-sectional profiles and friction loops are included in (d) and (e). The red dashed lines indicate the location and the corresponding normal force during the scratch test, where the cross-sectional profiles and friction loops are taken.

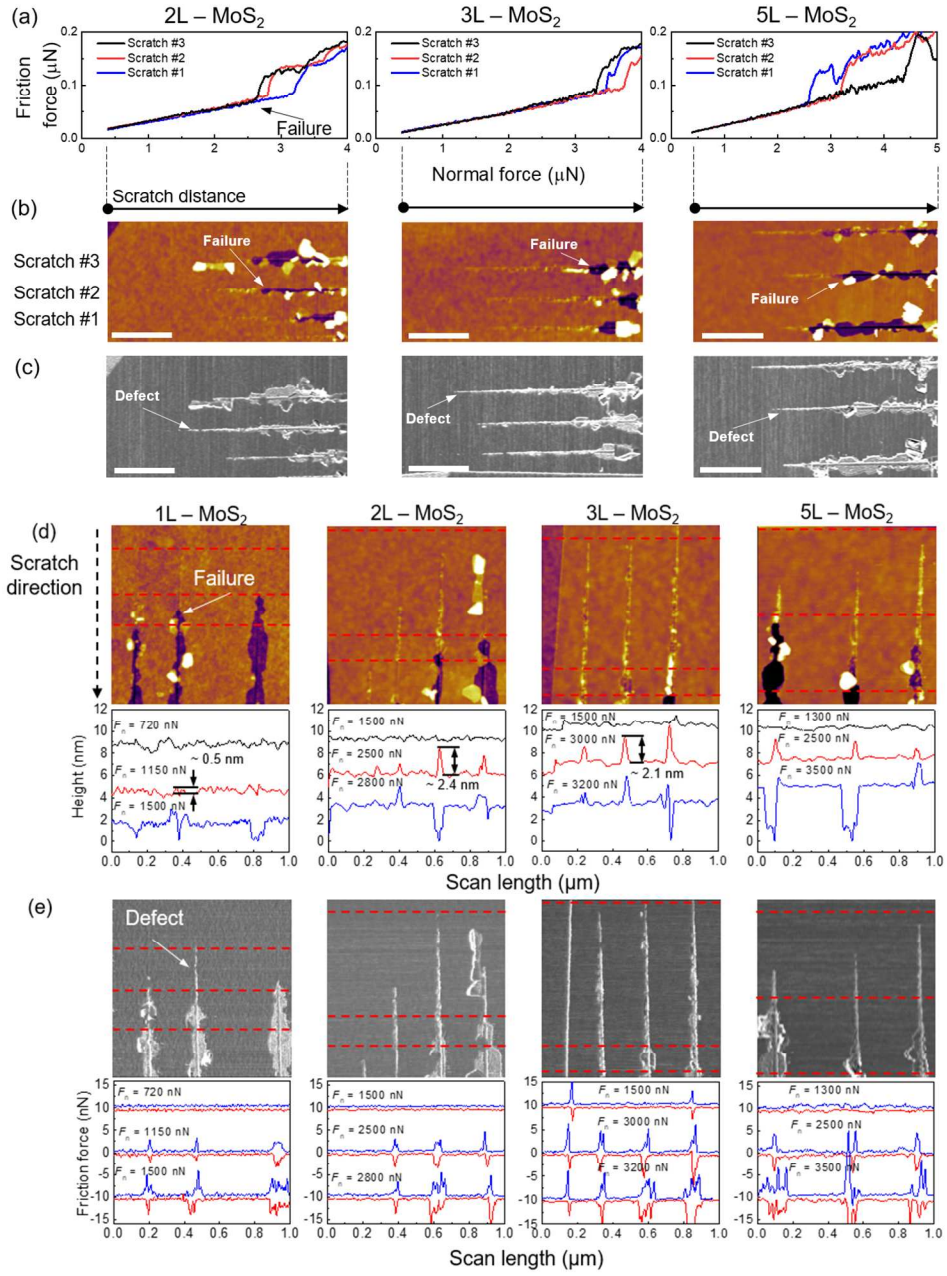

Figure S6. Progressive-force scratch test results for multi-layer MoS_2 specimens. (a) Friction force variation with respect to normal force, (b) topographic images, and (c) FFM images (forward scans) of scratch tracks after progressive-force scratch tests. In (b), the scratch distance of about 2 μm is noted. In (b) and (c), the scale bars are 500 nm. High-resolution (d) topographic images and (e) FFM images (forward scans) of scratch tracks formed at single- and multi-layer MoS_2 specimens after progressive-force scratch tests. The cross-sectional profiles and friction loops are included in (d) and (e). The red dashed lines indicate the location and the corresponding normal force during the scratch test, where the cross-sectional profiles and friction loops are taken.

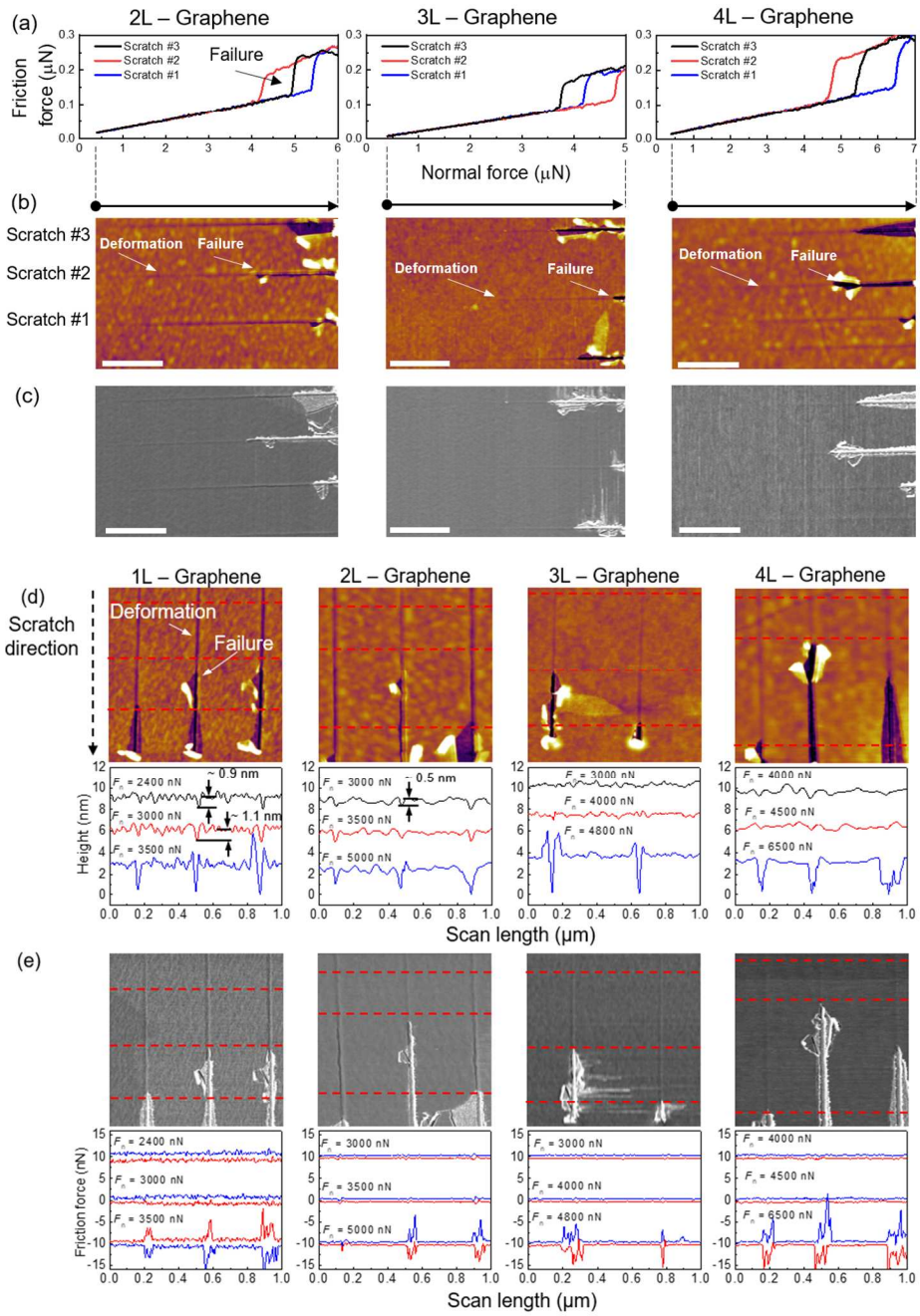

Figure S7. Progressive-force scratch test results for multi-layer graphene specimens. (a) Friction force variation with respect to normal force, (b) topographic images, and (c) FFM images (forward scans) of scratch tracks after progressive-force scratch tests. In (b), the scratch distance of about 2 μm is noted. In (b) and (c), the scale bars are 500 nm. High-resolution (d) topographic images and (e) FFM images (forward scans) of scratch tracks formed at single- and multi-layer graphene specimens after progressive-force scratch tests. The cross-sectional profiles and friction loops are included in (d) and (e). The red dashed lines indicate the location and the corresponding normal force during the scratch test, where the cross-sectional profiles and friction loops are taken.

6. Effect of number of layers on constant-force scratch tests

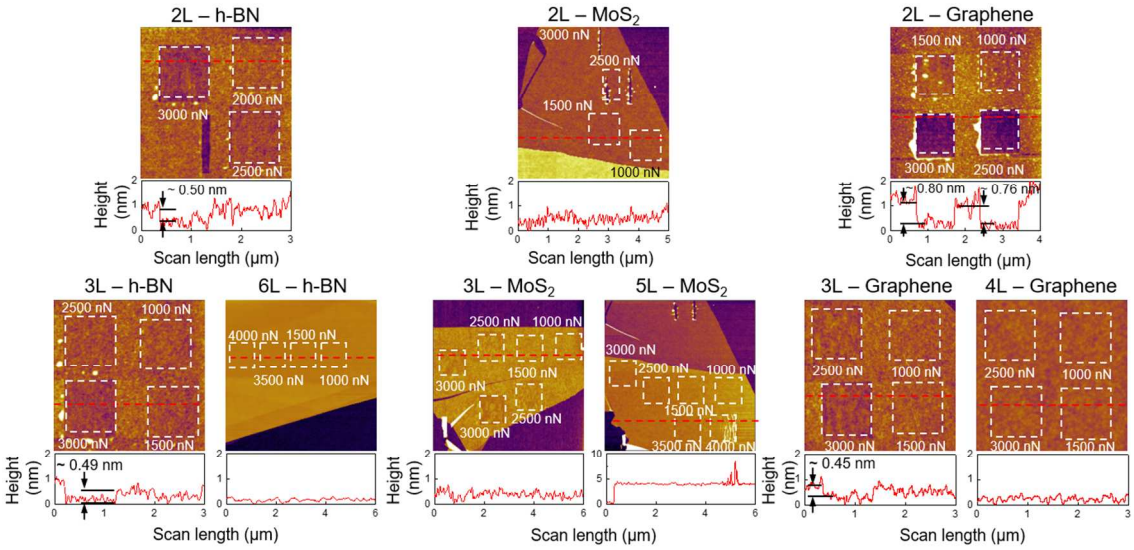

Figure S8. Topographic images of multi-layer h-BN, MoS_2, and graphene specimens after constant-force scratch tests. The cross-sectional profiles are included and the red dashed lines indicate the location where the cross-sectional profiles are taken. The scratched areas are depicted as white dashed boxes.

7. Adhesion forces before and after the scratch tests

The adhesion force between the diamond AFM tips and the atomically-thin h-BN, MoS_2 and graphene were compared before and after the scratch tests as an indirect means to monitor tip wear. The average adhesion force between the tip and specimens before and after scratch tests is shown in Figure S9. As shown, no significant changes in adhesion force were observed after the scratch tests, which suggests that tip wear during the scratch tests was negligible.[3]

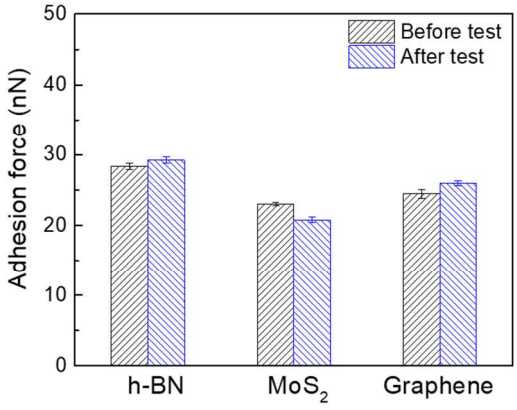

Figure S9. Adhesion force before and after the progressive and constant-force scratch tests. The error bars represent one standard deviation of the mean.

References

(1) Nan, H.; Wang, Z.; Wang, W.; Liang, Z.; Lu, Y.; Chen, Q.; He, D.; Tan, P.; Miao, F.; Wang, X.; Wang, J.; Ni, Z. Strong Photoluminescence Enhancement of MoS_2 through Defect Engineering and Oxygen Bonding. *ACS Nano* **2014**, 8, 5738-5745.

(2) Kim, Y.; Jhon, Y. I.; Park, J.; Kim, C.; Lee, S.; Jhon, Y. M. Plasma functionalization for cyclic transition between neutral and charged excitons in monolayer MoS_2. *Sci. Rep.* **2016**, 6, 21405.

(3) Chung, K. H. Wear characteristics of atomic force microscopy tips: A review. *Int. J. Precis. Eng. Man.* **2014**, 15, 2219-2230.